Energy 148 (2018) 112–122

Contents lists available at ScienceDirect

Energy

journal homepage: www.elsevier.com/locate/energy

A dimensionally reduced order piezoelectric energy harvester model

Shreya Banerjee, Sitikantha Roy*

Department of Applied Mechanics, Indian Institute of Technology-Delhi, New Delhi, 110016, India

ARTICLE INFO

Article history:
Received 19 January 2017
Received in revised form
22 January 2018
Accepted 24 January 2018
Available online 3 February 2018

Keywords:
Variational asymptotic method
Asymptotically correct model
Energy harvester
Piezoelectric material
Base excitation

ABSTRACT

Presently reduced power requirement for small electronic components have been the main motivation for developing vibration based energy harvesting. The ultimate objective in this research field is to provide an easy, sustainable and efficient technology to power such small electronic devices from the unused vibrational energy available in the environment. A comprehensive, reliable mathematical technique is thus in high demand which can model a piezoelectric energy harvester, predict its coupled dynamics (structural and electromechanical) accurately. The present work focuses on developing a mathematical model for a slender, piezoelectric energy harvester based on Variational Asymptotic Method, a dimensional reduction methodology. Variational Asymptotic Method approximates the 3D electromechanical enthalpy as an asymptotic series to formulate an equivalent 1D electromechanical enthalpy functional to perform a systematic dimensional reduction. For validation purpose, we have picked up experimental results for a bimorph PZT harvester, available in the literature. We have studied the extension-bending structural coupling along with the parameter dependence of the voltage, power output from the harvester and validated with the experiments. The present study provides a unique, accurate modeling technique which is capable of capturing material anisotropy, structural coupling and can analyse arbitrary cross section, surface mounted as well as embedded piezo layered energy harvester.

1. Introduction

In last few years there has been a surge of research in vibration based energy harvesting. The process of acquiring the unutilized energy from the surrounding and converting it into some usable form of energy is termed as energy harvesting. With the emerging miniature sized electronics and its various applicability in different domain, the need to power such devices with optimal maintenance has also increased [1]. Electromagnetic, electrostatic and piezoelectric are the three very basic energy conversion technique as stated in a very initial article by William and Yates [2]. It has also been mentioned that the significant advantage of piezoelectric material in energy harvesting as compared to the other two basic energy conversion mechanism i.e electromagnetic and electrostatic are its large power density and ease of application. A review article highlighting the advancement of power harvesting from piezoelectric materials was published by Anton and Sodano [3]. Also an article was published reviewing different strategies for increasing the operating frequency range of vibrating energy harvester [4].

The major advantage of piezoelectric material over other mentioned energy harvesting mechanisms is that voltage output can be directly obtained from piezoelectric material itself without any need of external powering source. Here voltage output emerges from the constitutive behaviour of the material. Also there is ease of fabrication of a piezoelectric material for both macro scale and micro scale level due to well established thick film and thin film techniques [5]. The energy conversion in the piezoelectric material occurs because of the orientation of the piezoelectric molecular structure which exhibit a local charge separation known as electric dipole. On application of strain energy there is deformation of dipole and simultaneously formation of charge that can be extracted from the material and can be used to power devices. The most typical type of energy harvester addressed in the literature are cantilever type energy harvester with one or more piezoceramic layer attached to it. Generally the harvester is attached to some vibrating base structure and dynamic strain is induced in piezoceramic layers resulting in alternating voltage output across the electrode. Also, an external resistive load is attached to the harvester structure. As an extension to the harvester structure a rectified bridge and a smoothing capacitor is used to convert the alternating voltage to stable rectified voltage which can be used for charging small electronics.

* Corresponding author.
E-mail address: sroy@am.iitd.ac.in (S. Roy).

https://doi.org/10.1016/j.energy.2018.01.116
0360-5442/

The most commonly used configuration in piezoelectric vibration based energy harvesting is a rectangular cantilever beam. Also multiple piezoelectric layers are added to improve power harvesting capabilities. Single piezoelectric layer in a harvester model is referred as unimorph, similarly two piezoelectric layer bonded to some substructure is termed as bimorph. Researchers have adopted both discrete [6] as well as distributed parameter approach to model unimorph [7] as well as bimorph structure as stated by Erturk et al. [8] and Aladwani et al. [9]. Piezoelectric materials can be configured in different ways to enhance power harvesting. Configuration can be changed by modifying the piezoelectric material by altering the electrode arrangement, changing the poling direction, tuning the natural frequency, adding tip mass etc [10]. Tip mass bimorph configuration was also studied by Wang et al. [11]. The selection of the type of piezoelectric material plays a vital role in influencing harvester performance. Another method for increasing the amount of energy harvested is through utilization of coupling mode. Tuning the harvester model at resonant frequency which matches the frequency of ambient vibrations is another way of improving the efficiency of piezoelectric energy harvester. Past literature suggests that depending on requirements the piezoceramic layers can be combined in series or parallel connection [12]. The electrical response of a series connection of piezoelectric energy harvester attached to various interface electronics including SSHI circuits were studied recently by Lin et al. [13]. Also comparison between series and parallel connection of the oscillators are made to show the significant differences.

Some of the early modeling techniques in piezoelectric energy harvester is lumped parameter single degree of freedom (SDOF) solution [14]. SDOF modeling is convenient as it used to consist of lumped parameters for both electrical and mechanical domain. Though this method was good enough to give an initial insight for any harvester model but it lacks the detail and in-depth analysis. Improved modeling approach was developed based on Rayleigh Ritz type discrete formulation by Hagood et al. [15] which was based on Hamilton's principle for electromechanical systems. This method proved to be more accurate approximation as compared to the previous method. Electrical output was represented analytically by Lu et al. [16]. But these analytical modeling oversimplified the piezoelectric coupling terms. A coupled piezoelectric circuit finite element model was developed to study the power output of the piezoelectric model connected with some external load by Zhu et al. [17]. Also an electromechanical finite element model for piezoelectric energy harvester plates was developed by Junior et al. [18]. Energy harvester with frame configuration was proposed by Soh et al. [19]. The harvester basically worked in two fundamental modes and is capable of capturing vibrational energy from arbitrary direction in 2D plane. Recently Hajati and Kim [20] proposed a wide bandwidth energy harvester model by exploiting the nonlinear stiffness of a doubly clamped MEMS resonator. A mechanical impact driven and frequency up converted wide bandwidth energy harvester model was developed theoretically and experimentally by Halim and Park [21]. It converts low frequency vibration from the environment into high frequency vibration by application of mechanical impact. The model shows potential application for small portable handheld wireless devices. It was discussed in some of the recent published literature sources that one of the critical disadvantages in designing a piezoelectric energy harvester is that they are being able to produce reasonable amount of power only when they are excited nearby to their fundamental natural frequencies. So some of the designing aspects were improved [22] like using an attached mass and segmented piezoelectric layer to get a broadband energy harvester. An analytical model for energy harvester named as phase-shift synchronous electric charge extraction was proposed by Lefeuvre et al. [23]. This model was mostly used to study the properties of control scheme in case of high and low electromechanical coupling. A finite difference model was proposed to model a tapered harvester and also estimating its efficiency [24]. It was shown that the model developed produces 70 times higher power than the uniform prismatic harvester model. An electromechanical model of a piezoelectric energy harvester with dual magnetic forces at its tip was studied for low frequency excitation problem [25]. To represent the magnetic force it is fitted into a fifth order polynomial representation. A two degree of freedom piezoelectric energy harvester was proposed by Hu et al. [26] with stopper which have a nonlinear dynamic interaction between the two degrees of freedom. The purpose of the proposed model is to have a robust performance over a wide frequency range which can be obtained if a harvester is insensitive to excitation frequencies.

Most of the energy harvester models discussed lack a generalized platform which can study material anisotropy, arbitrary cross sectional geometry and electromechanical coupling accurately in a single common platform. It can study harvesters operating in axial, bending or torsional mode or any combinations of them arising because of structural coupling. As most of the models have considered isotropic material so they have neglected the effect of structural coupling. Thus, most of the models proposed in literature are unable to capture the actual physics involved due to material anisotropy. A well-defined mathematical model is needed which can bridge these gaps. This research work will propose a rigorous mathematical technique known as Variational Asymptotic Method (VAM) to develop a generalized platform for energy harvester model which can account material anisotropy, structural coupling, and arbitrary cross sectional geometry and can calculate electromechanical coupling accurately.

Berdichevsky [27] introduced the theory Variational Asymptotic Method (VAM) in late 1970s. The theory has some inherent advantage such as systematic and easy numerical implementation without any priori kinematic assumptions [28]. VAM being a mathematically rigorous approach is applicable to study any real life structural problem inherently having some small parameters and which can be represented in totality by an energy functional. The method applies the asymptotic expansion to the energy functional instead of the system of differential equation which ultimately makes VAM less cumbersome as compared to the other standard asymptotic method. In the past, VAM has successfully established itself in the field of composite structures [29] as well as smart structures like beams [30] and rods [31]. VAM for modeling a sensor was established in our previous study [32]. The present work is to mathematically develop a piezoelectric energy harvester model using Variational Asymptotic Method (VAM). Fully coupled equation of motion was derived which is a new addition to the theory. Through this study we are also able to capture the coupled structural modes, structural coupling due to material anisotropy and coupling terms accurately.

The formulation initiates by defining an electromechanical enthalpy functional of a 3D structure. An asymptotically correct slender energy harvester model is developed. The concept of dimensional reduction lies entirely in identifying the inherently small parameters in the structure and then order estimation of the terms in the Hamiltonian. The elastodynamics of any structure is defined by a generalized Hamilton's principle as,

$$\int_{t_1}^{t_2} \left[\delta(T-U)+\overline{\delta W}\right] dt = 0 \tag{1}$$

where, t_1 and t_2 are arbitrary fixed times, T is the kinetic energy, U

is the electromechanical enthalpy and is the virtual work of applied loads and electric charges. The bar over the virtual work term defines that it need not be variation of functions or functional. A short schematic of the overall mathematical model has been shown in Fig. 1.

2. Mathematical model of an asymptotically correct piezoelectric energy harvester under base excitation

This section introduces the basic mathematical formulation involved. Global equations of motion have been derived for a fully coupled bimorph configured beam type energy harvester by Variational Asymptotic Method, which is a new addition to the present theory. The formulation initiates by defining the different terms associated in the Hamiltonian i.e the kinetic energy, potential energy, electrical energy and work done due to electrical and mechanical load. Derivation of coupled equation of motion for bimorph energy harvester under base excitation is explained based on defining the electromechanical enthalpy functional, estimating the terms by order estimation in the energy expression and solving a coupled structural dynamics problem under a steady state base vibration.

2.1. Kinematics: un-deformed and deformed configurations

2.1.1. Three dimensional description and development of strain field

A slender beam type structure is represented by a reference line and a reference cross section which is perpendicular to the reference line. At each point along the reference line an orthonormal triad $\boldsymbol{b}_i$ is introduced, which is tangent to $\boldsymbol{x}_i$. Thus any point in the un-deformed structure is then located by the position vector $\widehat{\boldsymbol{r}}$ which can be expressed as (see Fig. 2),

$$\widehat{\boldsymbol{r}}(x_1,x_2,x_3) = \boldsymbol{r}(x_1) + x_\alpha \boldsymbol{b}_\alpha \tag{2}$$

Similar expression for position vector of an arbitrary point on the deformed structure can be expressed as,

$$\widehat{\boldsymbol{R}}(x_1,x_2,x_3) = \boldsymbol{R}(x_1) + x_\alpha \boldsymbol{B}_\alpha(x_1) + \widehat{w}_i(x_1,x_2,x_3)\boldsymbol{B}_i(x_1) \tag{3}$$

Here $\boldsymbol{B}_i$ represents the new triad for a deformed state and can be related to an undeformed triad $\boldsymbol{b}_i$ as,

$$\boldsymbol{B}_i = \boldsymbol{C}^{Bb} \cdot \boldsymbol{b}_i \tag{4}$$

where $\boldsymbol{C}^{Bb}$ is the rotation tensor. In the absence of deformations $\boldsymbol{B}_i$ coincides with $\boldsymbol{b}_i$. $\widehat{w}_i$ are known as the warping functions which allows all other possible cross sectional deformations.

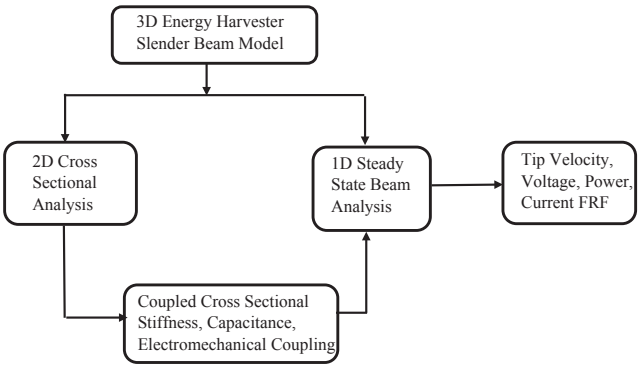

Fig. 1. Brief methodology.

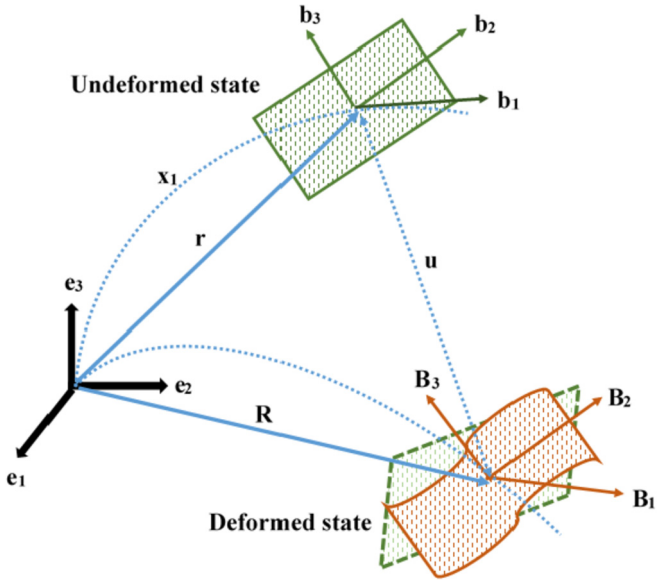

Fig. 2. Deformation of a cross section.

By using the 3D space curve definition from the Frenet's description we can write,

$$\begin{aligned} \boldsymbol{b}_i' &= \boldsymbol{k} \times \boldsymbol{b}_i \text{ where, } \boldsymbol{k} = k_j \boldsymbol{b}_j \\ \boldsymbol{B}_i' &= \boldsymbol{K} \times \boldsymbol{B}_i \text{ where, } \boldsymbol{K} = K_j \boldsymbol{B}_j \end{aligned} \tag{5}$$

$\boldsymbol{k}$ represents the initial curvature vector, $\boldsymbol{K}$ is the total curvature vector. $\boldsymbol{K}$ can be expressed as the sum of initial curvature vector and elastic curvature κ [33].

Mixed basis component of deformation gradient tensor is obtained from covariant and contravarient base vectors. Covarient base vectors are tangent to the coordinate curves which is mathematically expressed as [33],

$$\boldsymbol{g}_i = \frac{\partial \mathbf{r}}{\partial x_i} \text{for undeformed and } \boldsymbol{G}_i = \frac{\partial \mathbf{R}}{\partial x_i} \text{for deformed} \tag{6}$$

Contravarient base vector are normal to the coordinate surfaces and defined as,

$$\boldsymbol{g}^i = \frac{1}{2\sqrt{g}} \boldsymbol{e}_{ijk}\left(\boldsymbol{g}_j \times \boldsymbol{g}_k\right) \text{ where } g = \det\left(\boldsymbol{g}_i \cdot \boldsymbol{g}_j\right) \tag{7}$$

Thus the mixed basis component of deformation gradient tensor can be calculated as,

$$F_{ij} = \boldsymbol{B}_i \cdot \boldsymbol{G}_k \boldsymbol{g}^k \cdot \boldsymbol{b}_j \tag{8}$$

2.1.2. Jaumann Biot Cauchy strain tensor

In the present work the local rotations and displacements considered are small so the strain tensor can be expressed by linear Jaumann Biot Cauchy strain tensor which are valid for small strains and can be defined as,

$$\Gamma_{ij} = \frac{1}{2}(F_{ij} + F_{ji}) - \delta_{ij} \tag{9}$$

where δ_{ij} is the Kronecker symbol, and F_{ij} is the mixed-basis component of the deformation gradient tensor as defined in equation (8).

It is essential to express 3D strain field in terms of 1D

generalized strain which are treated as unknowns for a 1D beam type harvester model. The 1D generalized strains are defined as,

$$\begin{aligned}\gamma_{11}\boldsymbol{b}_1 &= \boldsymbol{b}_i\boldsymbol{B}_i\cdot\boldsymbol{R}' - \boldsymbol{r}'\\ \kappa_i\boldsymbol{b}_i &= \boldsymbol{b}_i\boldsymbol{B}_i\cdot\boldsymbol{K} - \boldsymbol{k}\end{aligned} \tag{10}$$

In equation (10) $\boldsymbol{\gamma}$ represents the force strain vector and $\boldsymbol{\kappa}$ represents the moment strain vector in the b-basis. The matrix form of 1D strains for Euler Bernoulli beam type energy harvester model is given as,

$$\gamma = \{\,\gamma_{11} \quad 0 \quad 0\,\}^T \quad \text{and} \quad \kappa = \{\,\kappa_1 \quad \kappa_2 \quad \kappa_3\,\}^T \tag{11}$$

All these strain measures come as conjugates to 1D sectional force resultants in the 1D variational statement. Apart from mechanical field any electromechanical structure consists of electric field. The electric field E is characterised by electric potential $\tilde{\phi}$. Thus by definition we can write,

$$\boldsymbol{E} = -\nabla\tilde{\varphi} = -\frac{\partial\tilde{\varphi}}{\partial x_i}\boldsymbol{g}^i \tag{12}$$

where, $\boldsymbol{g}^i$ are the contravarient base vectors.

Combining both mechanical and electrical field we can introduce a complete 3D strain vector as,

$$\Gamma = [\Gamma_{11} \;\; 2\Gamma_{12} \;\; 2\Gamma_{13} \;\; \Gamma_{22} \;\; 2\Gamma_{23} \;\; \Gamma_{33} \;\; E_1 \;\; E_2 \;\; E_3]^T \tag{13}$$

From equation (9) and equation (12) we can get the linear expression of 3D strain field in terms of 1D strains and warping vector as,

$$\boldsymbol{\Gamma} = \boldsymbol{\Gamma}_h\widehat{w} + \boldsymbol{\Gamma}_\varepsilon\varepsilon \tag{14}$$

where, $\boldsymbol{\Gamma}_h$ and $\boldsymbol{\Gamma}_\varepsilon$ are the 9×4 operator matrix as referred in Roy et al. [30].

The 1D strain vector and warping vector for an Euler-Bernoulli type harvester model are expressed as,

$$\varepsilon = [\gamma_{11} \;\; \kappa_1 \;\; \kappa_2 \;\; \kappa_3]^T \;\text{ and }\; \widehat{w} = [w_1 \;\; w_2 \;\; w_3 \;\; \phi]^T \tag{15}$$

2.2. Constraints on warping field

To solve reduced order beams with arbitrary cross section by Variational Asymptotic Method (VAM) we need some numerical method in combination. So finite element method (FEM) is used along with VAM to discretise the unknown warping field and the induced electric potential over the cross section. Discretised form of the warping field can be expressed as,

$$\widehat{w}(x_1,x_2,x_3) = S^u(x_2,x_3)V(x_1) \tag{16}$$

where, S^u is the element shape function and is of $4\times 4n$ dimension, n being the number of nodes in the element. V refers to the nodal values of the warping and of dimension $4n\times 1$. The global constraints on warping function was derived from the fact that warping should not contribute to the rigid body displacements.

A valid warping field should not contribute to the rigid body type motion of a cross-section and can be realized if following integral constrains are invoked.

- $\langle w_1\rangle = 0$, $\langle w_2\rangle = 0$ and $\langle w_3\rangle = 0$, represents 3 constraints on rigid body translational displacements.
- $\langle x_2w_3 - x_3w_2\rangle = 0$, represent constraint on global rotation in the 2–3 plane i.e cross sectional plane.

The total nodal values of the warp field for any arbitrary cross section are divided into two parts such as,

$$V = V_k + V_u \tag{17}$$

here V_k is the known electric potential matrix at specific points (nodes) and V_u is the unknown induced electric potential matrix. The detailed has been discussed in our previous published work on sensor model [32].

3. Kinetic energy, strain energy and work done

3.1. Kinetic energy

The kinetic energy can be directly calculated from the absolute velocity of the generic point in the structure. It can be mathematically expressed by taking a time derivative of equation (3), for details refer Roy et al. [30].

$$\vartheta = \vartheta_o + \Omega(\xi + w) + \dot{w} \tag{18}$$

where, ϑ_o is the absolute velocity of a point in the deformed reference line, Ω is the inertial angular velocity of $\boldsymbol{B}_i$ bases, $\xi = [0 \;\; x_2 \;\; x_3]^T$ and $\dot{w}$ denotes the partial derivative with respect to time. In equation (18) $\vartheta, \vartheta_o, \Omega, w$ denotes column matrices containing the components of corresponding vectors in $\boldsymbol{B}_i$ bases. The kinetic energy can be expressed as,

$$\begin{aligned}T &= \frac{1}{2}\int_V \rho\vartheta^T\vartheta dV\\ \text{Also,}\quad T &= T_{1D} + T^*\end{aligned} \tag{19}$$

T_{1D} is the portion of kinetic energy which is not related to the 3D unknown warping functions $\widehat{w} = [w_1 \;\; w_2 \;\; w_3 \;\; \varphi]^T$, ρ is the mass density and v is the absolute velocity of any point in the structure. T^* contains the unknown 3D functions of higher order.

3.2. Strain energy

The strain energy can be written assuming the material is linearly elastic. Thus for such material the 3D stress and strain tensors are related to each other by generalized Hook's law as,

$$\sigma = C\Gamma \tag{20}$$

Here, C is the matrix of elastic material property.

The strain energy expression for piezoelectric material as already mentioned in Ref. [30] is,

$$U = \frac{1}{2}\int_v \left(\Gamma^T : C^E : \Gamma - 2E\cdot e : \Gamma - E^T\cdot\varepsilon^\Gamma\cdot E\right)dv \tag{21}$$

where, e, ε^Γ and C^E are matrices constituting piezoelectric coupling, dielectric matrix at constant strain and elastic property matrix at constant electric field. From equation (21) the strain energy can be expressed as,

$$U = \frac{1}{2}\int_0^L \left\langle \Gamma^T\begin{bmatrix}C^E & -e^T\\ -e & -\varepsilon^\Gamma\end{bmatrix}\Gamma\sqrt{g}\right\rangle dx_1 \equiv \frac{1}{2}\int_0^L \left\langle \Gamma^T C\Gamma\sqrt{g}\right\rangle dx_1 \tag{22}$$

where L denotes the length of the beam. The angle brackets symbolizes integration over the cross-sectional plane.

3.3. Work done

If no electric charges applied on the surfaces or inside the body, the virtual work of the active beam is completely done by applied loads and can be calculated as [30],

$$\delta\overline{W} = \int_0^L \left(\langle F \cdot \delta\widehat{R}\sqrt{g} \rangle + \oint_{\partial\Omega} Q \cdot \delta\widehat{R} ds \right) dx_1 + \langle Q \cdot \delta\widehat{R} \rangle \tag{23}$$

where $\partial\Omega$ denotes the lateral surface of the beam, $F = F_i B_i$ are the applied body forces and $Q = Q_i B_i$ are the applied surface tractions. $\delta\widehat{R}$ denotes the Lagrangian variation of the displacement field i.e, $\delta\widehat{R} = \delta q_i B_i + x_\alpha \delta B_\alpha + \delta\widehat{w}_i B_i + \widehat{w}_j \delta B_j$ where the virtual displacement and rotation are defined as, $\delta\overline{q}_i = \delta\widehat{R} \times B_i$ and $\delta B_i = \delta\overline{\varphi}_j B_j \times B_i$.

Here $\delta\overline{q}_i$ and $\delta\overline{\varphi}$ contain the components of virtual displacement and rotation in the B_i system. As the warping functions are small, one can ignore the products of warping and virtual rotation in $\delta\widehat{R}$ and obtain virtual work due to applied loads as,

$$\delta\overline{W} = \delta\overline{W}_{1D} + \delta\overline{W}^* \tag{24}$$

$\delta\overline{W}_{1D}$ is the virtual work containing only functions of x_1 not related to the warping function $\widehat{w}_i(x_1, x_2, x_3)$ and δW^* is the virtual work related with the 3D warping functions and their time derivatives.

4. Reformulated Hamilton's principle

Hamilton's principle from equation (1) may be reformed and rewritten as,

$$\int_{t_0}^{t_1} \left(\delta \int_0^L (T_{1D} + T^*) dx_1 - \delta \int_0^L (\langle U_{3D} \rangle + U^*) dx_1 - \left(\delta\overline{W}_{1D} + \delta\overline{W}^* \right) \right) dt = 0 \tag{25}$$

The complexity in solving equation (25) is same as solving any 3D problem which are due to the unknown 3D warping function in the electromechanical strain energy expression. Variational asymptotic method (VAM) provides a powerful mathematical technique to solve the unknown 3D warping functions by asymptotic expansion of the variational statement of electromechanical strain energy expression.

$$\delta U = 0 \tag{26}$$

The process of reducing 3D variational statement to a 1D Hamiltonian is called the dimensional reduction.

5. Dimensional reduction from 3D to 1D

Dimensional reduction can be done approximately by taking advantage of the inherent small parameters present in the structure. It makes the whole process time efficient without any loss in accuracy.

5.1. Small parameters

The fundamental concept behind the present theory lies in dimensionally reducing a structure, for a beam like structure it will be reduction from a 3D to 1D structure by taking advantage of the slenderness ratio. The small parameters considered are:

- Strains: The present study focuses on materially linear theory but can accommodate geometrical nonlinearity. Such condition defines the working condition of the structure restricts the 3D and 1D strain fields to be small. This defines, which should be such that it always induce strains of small magnitude.
- $\frac{h}{l}$ ratio: $\frac{h}{l}$ ratio represents the slenderness ratio where h is the characteristic size of the cross section, l denotes the characteristic wavelength of axial deformation. Thus $\overline{h} = \frac{h}{l} << 1$ should satisfy to be modelled as a beam structure.

5.2. Order estimation

Order estimation gives us an idea about the relative orders of the terms in the strain expression subsequently in the energy expressions. As the present analysis the strain is small, so the order of magnitude of strain can be expressed as,

$$\overline{\varepsilon} \sim O(\varepsilon) \sim O(\Gamma) << 1 \tag{27}$$

$\overline{\varepsilon}$ denotes the maximum strain the material can withstand for the present study. We can also estimate $x_\alpha \sim O(h)$ and $k_i \sim O\left(\frac{1}{R}\right)$ where R is the characteristic radius of curvature or twist of the beam type harvester model.

From equation (14) and also considering the above order estimation we can obtain the relative order magnitudes of other quantities,

$$\gamma_{11} \sim O(\varepsilon), h\kappa_i \sim O(\varepsilon) \quad \text{and} \quad w_i \sim O(h\varepsilon) \tag{28}$$

Therefore, the order estimation for zeroth order 3D strain will be,

$$\left(\Gamma_h \widehat{w} + \Gamma_\varepsilon \varepsilon \right) \sim O(\varepsilon) \tag{29}$$

The strain energy density U will be of order $\mu\overline{\varepsilon}^2$ where μ denotes the order of elastic constants. The other terms in the Hamiltonian i.e the virtual work and the kinetic energy are of same order as strain energy. The orders for applied forces and moments for a Euler-Bernoulli type harvester model can be estimated as,

$$F_1 \sim O\left(\frac{\mu\overline{h}\varepsilon}{h}\right), Q_1 \sim O\left(\mu\overline{h}\varepsilon\right), F_\alpha \sim O\left(\frac{\mu\overline{h}^2\varepsilon}{h}\right), Q_\alpha \sim O\left(\mu\overline{h}^2\varepsilon\right) \tag{30}$$

For low frequency energy harvester vibration,

$$\frac{h}{c_s \tau} \sim O\left(\overline{h}\right) << 1 \tag{31}$$

τ represents the scale of change of displacement and warping functions in time and $c_s = \sqrt{\frac{\mu}{\rho}}$ is the characteristic velocity of shear waves [30].

5.3. Asymptotic analysis

The asymptotic analysis is based on identifying the small parameters in the structure and also by order estimation of the strain energy expression.

The asymptotic expansion of the strain energy per unit length in terms of small parameters indentified in the structure can be expressed as,

$$2U = 2U_0 + 2U_1 + 2U_2 + 2U_3 + \ldots \tag{32}$$

where, $2U_0 \rangle 2U_1 \rangle 2U_2 \rangle 2U_3 \ldots$

Zeroth order: It considers only leading order terms upto $\mu\varepsilon^2$ in strain energy expression. Present study is completely based on zeroth order estimation.

First order: The zeroth order solution is perturbed for warping and substituting it into the strain energy expression upto order of $\mu\bar{h}\varepsilon^2$.

Second order: Order upto $\mu\bar{h}^2\varepsilon^2$ terms are kept in the strain energy expression.

Substituting Eq. (16) into Eq. (22) along with Eq. (14) we obtain the expression for zeroth order approximation for electromechanical enthalpy as,

$$2U_0 = V^T E V + 2V^T D_{h\varepsilon}\varepsilon + \varepsilon^T D_{\varepsilon\varepsilon}\varepsilon \tag{33}$$

where, $E = \langle [\Gamma_h S^u]^T C [\Gamma_h S^u] \rangle$, $D_{h\varepsilon} = \langle [\Gamma_h S^u]^T C [\Gamma_\varepsilon] \rangle$ and $D_{\varepsilon\varepsilon} = \langle [\Gamma_\varepsilon]^T C [\Gamma_\varepsilon] \rangle$. Applying constraints and solving equation (33) as given in Roy et al. [30] we finally end up getting the zeroth order generalized approximation of fully coupled electric enthalpy,

$$2U_0 = \varepsilon^T \left(\widehat{V}_0^T D_{h\varepsilon} + D_{\varepsilon\varepsilon} \right) \varepsilon + \varepsilon^T \left(\widehat{V}_0^T E V_k + D_{h\varepsilon}^T V_\phi + 2 D_{h\varepsilon}^T V_k \right) + \left(V_\phi^T E V_k + V_k^T E V_k \right) \tag{34}$$

or, we can also represent equation (34) as a thermodynamically consistent 1D enthalpy,

$$2U_0 = \varepsilon^T S \varepsilon - 2\varepsilon^T f^a \phi - c_p \phi^2 \tag{35}$$

where S is the cross sectional stiffness of the electromechanical system, f^a is the electromechanical coupling coefficient and c_p is the capacitance per unit length of the structure. The 1D coupled constitutive equations of the energy harvester model which relates 1D generalized resultant forces on the harvester cross section with the 1D generalized strains as well as voltage,

$$F = \frac{\partial U}{\partial \varepsilon}, \quad \text{or,} \quad F = S\varepsilon - f^a \phi \tag{36}$$

and,

$$q = \frac{\partial U}{\partial \phi}, \quad \text{or,} \quad q = -\varepsilon^T f^a - c_p \phi \tag{37}$$

Equations (36) and (37) represents the coupled cross-sectional equations for the energy harvester model.

6. Short circuit and open circuit condition

Short or closed circuit condition is referred to as when the external load or electrical resistance is very low. And closed circuit condition is when the external load or electrical resistance is very high. The two circuit conditions are important to study for an energy harvester model to know about the minimum and maximum operating range of the model. When we solve a free vibration problem for an energy harvester we get two different natural frequencies corresponding to the short circuit and closed circuit conditions.

6.1. Short circuit or closed circuit condition

The short circuit condition at the cross sectional level will be represented by the following equation,

$$\dot{q} = i = \frac{\phi}{R} = -\dot{\varepsilon}^T f^a - c_p \dot{\phi} \tag{38}$$

Since, $R \to 0$ so the coupled cross sectional equation will be,

$$F = S\varepsilon \tag{39}$$

6.2. Open circuit condition

The open circuit condition at the cross sectional level will represent,

$$0 = -\dot{\varepsilon}^T f^a - c_p \dot{\phi} \tag{40}$$

Substituting equation (40) in equation (36) and integrating it we get the corrected cross sectional stiffness for the open circuit condition as,

$$\overline{S} = S + \frac{f_a \cdot f_a^T}{c_p} \tag{41}$$

Thus the coupled cross sectional equation for open circuit condition $(R \to \infty)$ will be,

$$F = \overline{S}\varepsilon$$

$$0 = -\dot{\varepsilon}^T f^a - c_p \dot{\phi} \tag{42}$$

7. Coupled finite element model with base excitation and tip mass

From equation (20), neglecting the higher order kinetic energy terms (T^*) we can express T_{1D} as

$$T_{1D} = \frac{1}{2} \sum_{e=1}^{N} \left(\left\{ \left\{ \dot{\delta}_e \right\} + \left\{ \dot{\delta}_{eBase} \right\} \right\}^T [M_b + M_t] \left\{ \left\{ \dot{\delta}_e \right\} + \left\{ \dot{\delta}_{eBase} \right\} \right\} \right) \tag{43}$$

where $\{\delta_e\}$ is the nodal deflection vector of beam element relative to the base fixed coordinate system for 2-noded single element and $\{\delta_{eBase}\}$ is the displacement vector for the translating base and are represented as,

$$\{\delta_e\} = \left\{ u_1^1 \quad \theta^1 \quad u_3^1 \quad \varphi_1^1 \quad u_2^1 \quad \varphi_2^1 \quad u_1^2 \quad \theta^2 \quad u_3^2 \quad \varphi_1^2 \quad u_2^2 \quad \varphi_2^2 \right\} \tag{44}$$

$$\text{and,} \quad \{\delta_{eBase}\} = \left\{ w_{b1}^1 \;\; 0 \;\; w_{b2}^1 \;\; 0 \;\; w_{b3}^1 \;\; 0 \;\; w_{b1}^2 \;\; 0 \;\; w_{b2}^2 \;\; 0 \;\; w_{b3}^2 \right\} \tag{45}$$

Here, u_i^P: P th node, $i = 1, 2, 3$ displacements, φ_i^P : P th node, $i = 1, 2, 3$ rotations, $w_{b_i}^P$: base displacements along 1, 2, 3 directions.

$$[M_b] = \int_0^{l_e} m_t \{N\}^T \{N\} dx_1 \tag{46}$$

$m_t = m_s + 2m_p$ is total mass per unit length for a bimorph configuration and M_b is the elemental mass matrix of bimorph beam. m_s and m_p are the mass per unit length of the substructure and piezo layer.

$$M_t = \{a\}^T m_t \{a\} \tag{47}$$

where, M_t is due to the tip mass, and $\{a\} = \{0\ 0\ 0\ 0\ 0\ 0\ 1\ 0\ 1\ 0\ 1\ 0\}$ as tip mass will contribute to all translating degree of freedom for the last node of last element in the harvester. So global mass matrix of the harvester is $M = \sum_{e=1}^{N} M_b + M_t$.

Potential Energy (U): The total potential energy or strain energy of an asymptotically correct energy harvester can be expressed as,

$$U = \frac{1}{2}\int_V \varepsilon^T \sigma d\nu \tag{48}$$

Now substituting equation (36) in equation (48) we get,

$$U = \frac{1}{2}\int_0^{l_e} \varepsilon^T (S\varepsilon - f^a \phi(x,t)) dx_1 \tag{49}$$

Finally the potential energy term with the electromechanical coupling term as,

$$U = \frac{1}{2}\int_0^{l_e} \{\delta_e\}^T [B]^T S[B]\{\delta_e\} dx_1 - \frac{1}{2}\int_0^{l_e} \{\delta_e\}^T [B]^T f^a \phi(x,t) dx_1 \tag{50}$$

here, $[B]$ is the strain displacement matrix.

Electrical Energy (E): The electrical energy expression can be obtained from,

$$W_{ee} = \sum_{e=1}^{n} \frac{1}{2}\left(\int_\nu E_3 D_3 d\nu_p\right) \tag{51}$$

$$\text{or,}\quad W_{ee} = \sum_{e=1}^{n}\left(\frac{1}{2}\int_0^{l_e} \phi q\, dx_1\right) \tag{52}$$

where, q is the charge per unit length.

Now taking the variation of the energy expression as given in equation (35) with respect to voltage we get the electrical equation as,

$$\frac{\partial U_0}{\partial \phi(x,t)} = -\varepsilon^T f^a - c_p \phi(x,t) \tag{53}$$

Thus substituting equation (53) in equation (52),

$$W_{ee} = -\frac{1}{2}\int_0^{l_e} \phi(x,t)\{\delta_e\}^T [B]^T f^a dx_1 + \frac{1}{2}\int_0^{l_e} c_p \phi(x,t)^2 dx_1 \tag{54}$$

The first term denotes the coupling term in the electrical energy expression.

Generalized Hamiltonian for piezoelectric energy harvester:

For an electromechanical structure the generalized Hamilton's principle can be expressed as,

$$\int_{t_1}^{t_2} \left[\delta(T - (U - W_{ee})) + \overline{\delta W}\right] dt = 0 \tag{55}$$

$$\text{where,}\quad \delta\overline{W} = \int_0^L \left(\langle F \times \delta\widehat{R}\sqrt{g}\rangle + \oint_{\partial\Omega} Q \times \delta\widehat{R} ds\right) dx_1 + \langle Q \times \delta\widehat{R}\rangle \tag{56}$$

is the work done due to the mechanically applied and electrically extracted work. By substituting each term in the generalized Hamiltonian and performing the variation we get the coupled dynamic equation of an energy harvester as,

$$M\left\{\ddot{\delta}\right\} + C\left\{\dot{\delta}\right\} + K\{\delta\} - \vartheta\phi(x,t) = -M\left\{\ddot{\delta}_{base}\right\}$$
$$\text{and,}\quad C_p\dot{\phi}(x,t) + \frac{\phi}{R} + \vartheta\left\{\dot{\delta}\right\} = 0 \tag{57}$$

Equation (57) is the global equation of motion where M, C and K are the global mass, damping and stiffness matrix of the harvester. ϑ and C_p are the system coupling vector and total capacitance. The damping for the present analysis is assumed to be proportional damping as,

$$C = \alpha M + \beta K \tag{58}$$

α and β are the constant of proportionality.

The short circuit and open circuit natural frequency can be obtained by solving the simple eigen value problem.

The equation of motion for short circuit condition will be,

$$[K] - \omega^2[M] = 0 \tag{59}$$

and for open circuit condition will be,

$$[K] - \omega^2[M] + \frac{[\vartheta][\vartheta]^T}{C_p} = 0 \tag{60}$$

In a bimorph configuration the electrode pairs covering each piezoceramic layer can be connected either in series or in parallel to the external load to get larger voltage or current output. Generally piezoceramic layers have opposite poling direction and also when the voltage drop in the whole structure is the summation of voltage drop in each piezo layer then it is termed as a series connection and when voltage drop in the whole structure is equal to the voltage drop in each piezo layer and also have same poling direction then the circuit arrangement is parallel connection (Fig. 3). Also the

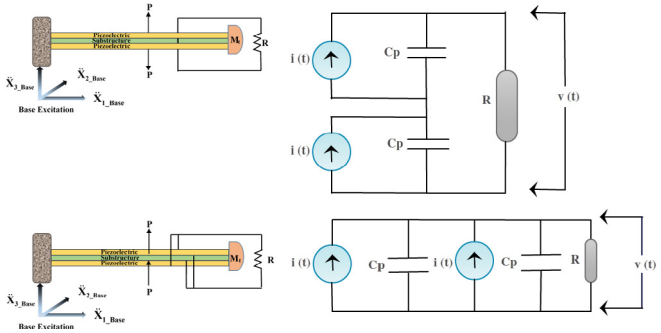

Fig. 3. Electrical circuit representation of series connection and parallel connection of bimorph energy harvester.

effective electromechanical coupling vector and effective capacitance is the sum of each individual layer for a parallel connection. For series connection the effective electromechanical coupling vector is equal to one piezoceramic layer and effective capacitance is half of the capacitance of one piezoceramic layer.

8. Steady state formulation for a harmonic base excitation

For a harmonic base excitation or any harmonic vibration coming from environment let the mathematical form of base displacement be, $x_b = X_B e^{j\omega t}$ (X_B is the amplitude, ω is the excitation frequency and x_b the base displacement),

So considering such voltage FRF can be derived as given in equation (61),

$$\phi_{FRF} = \frac{-j\omega\left(\frac{1}{R}+j\omega C_p\right)^{-1}\vartheta^T\left[-\omega^2 M+j\omega C+K+j\omega\left(\frac{1}{R}+j\omega C_p\right)^{-1}\vartheta\vartheta^T\right]^{-1}MX_B}{X_B} \tag{61}$$

The tip velocity FRF is the ratio of velocity amplitude at the tip with respect to the inertial or fixed reference frame to the gravitational acceleration is,

9. Case study

In this section we try to model and study a cantilever bimorph energy harvester with a tip mass under a harmonic base excitation. The Frequency Response Functions (FRFs) for tip velocity, voltage, current and power outputs are studied using the electromechanical formulation discussed earlier and also validated with the experimental results published by Ertuk et al. [8] in the year 2009. The input to the system is considered as a harmonic base acceleration. The piezoelectric bimorph structure is made up of two layers of PZT 5A bonded by a substructure brass. A tip mass is added to the structure for frequency tuning. The bimorph is clamped to the base structure at one end like a cantilever. The geometrical and material properties are mentioned in Table 3. The proposed theory is capable of capturing structural coupling which is neglected in most of the published literature sources. Most of the literature sources on energy harvesting determines the electrical power produced from bending vibration only. The cross sectional model as given in equation (66) in the present study has four degree of freedom per node which are axial, torsion, bending in x_3 direction and bending in x_2 direction. The corresponding strains are axial strain (γ_{11}), torsional strain (κ_1), bending strain in x_3 direction (κ_2) and bending strain in x_2 direction (κ_3).

$$\begin{bmatrix} F_1 \\ M_1 \\ M_2 \\ M_3 \end{bmatrix} = \begin{bmatrix} s_{11} & s_{12} & s_{13} & s_{14} \\ s_{12} & s_{22} & s_{23} & s_{24} \\ s_{13} & s_{23} & s_{33} & s_{34} \\ s_{14} & s_{24} & s_{34} & s_{44} \end{bmatrix} \begin{bmatrix} \gamma_{11} \\ \kappa_1 \\ \kappa_2 \\ \kappa_3 \end{bmatrix} - \begin{bmatrix} f_1^a \\ m_1^a \\ m_2^a \\ m_3^a \end{bmatrix} \phi(x,t), \quad \text{and} \quad -q = \{\gamma_{11} \;\; \kappa_1 \;\; \kappa_2 \;\; \kappa_3\} \begin{bmatrix} f_1^a \\ m_1^a \\ m_2^a \\ m_3^a \end{bmatrix} + c_p\phi(x,t) \tag{66}$$

$$w_{abs} = -\frac{j}{\omega}(1+X_0) \tag{62}$$

$$\text{where, } X_0 = \left[-M\omega^2 + Cj\omega + K + j\omega\left(j\omega C_p + \frac{1}{R}\right)^{-1}\vartheta\vartheta^T\right]^{-1} M\omega^2 X_B \tag{63}$$

Current FRF can be expressed as,

$$I_{FRF} = \frac{\phi_{FRF}}{R} \tag{64}$$

and, power FRF can be obtained as,

$$P_{FRF} = \frac{\phi_{FRF}^2}{R} \tag{65}$$

The equivalent coupled cross sectional stiffness constants as given in equation (66), are calculated and given in Table 1. The cross sectional stiffness shows a significant axial-bending structural coupling (i.e s_{13} coupling) under a harmonic base vibration. This term is interesting, as it entirely arise because of the presence of electro-mechanical coupling. The experimental beam layups is a symmetric arrangement structurally, and hence should not show any extension-bending structural coupling in the absence of electromechanical coupling. Simultaneously the axial-bending structural coupling reduces if we consider plane stress material property which is a significant assumptions in most of the theories for same harmonic base vibration. For experimental validation purpose we have considered the work of Erturk et al. [8]. Also we have considered plane stress material property for the experimental validation for our present study because the geometry of the harvester considered in the published work of Erturk et al. [8] is a strip or plate kind of structure rather a slender beam type of structure. A tabular comparison and validation of the electrical and mechanical properties for both 3D and plane stress material property has been shown in Table 1. And also our present study is

Table 1
Comparison of cross sectional constants (S matrix) and electromechanical constants with three dimensional material property and plane stress material property of bimorph energy harvester obtained from VAM and work done by Erturk et al. [9].

Equivalent structural and circuit parameters	VAM with 3D material property	VAM with plane stress material property	Erturk et al. [9]
s_{11}(N)	0.15589551E+07	0.15589551E+07	–
s_{13}(Nm)	0.35813669E-03	0.24158341E-05	–
s_{22}(Nm^2)	0.68846980E-01	0.68846980E-01	–
s_{33}(Nm^2)	0.51187423E-01	0.51324480E-01	0.50566e-01
s_{44}(Nm^2)	0.13137307E+03	0.13137306E+03	–
Capacitance (C_P)	6.7255E-07	5.8729E-07	8.1640E-07
Electromechanical coupling (m_2^a)	2.1794E-05	6.6144E-05	6.6144E-05

Table 2
Comparison between electrical and mechanical characteristics of bimorph configured energy harvester for series and parallel connection.

Equivalent structural and circuit parameters	Series connection	Parallel connection
Bending stiffness (S_{33})	5.13244E-02	5.1330906E-02
Axial-bending structural coupling (S_{13})	0.24601848E-11	−0.42338857E-08
Equivalent capacitance per unit cross section (C_P)	5.8729E-07	2.3491E-06
Electromechanical coupling (m_2^a)	6.6144E-05	0.13284912E-03

Table 3
Geometric properties of bimorph energy harvester with tip mass.

	PZT 5A	Brass
Length (L) m	.0508	.0508
Width (b) m	.0318	.0318
Thickness (m)	.00026	.00014
Piezoelectric constant e_{31} (C/m^2)	−10.4	–
Dielectric constant ε_{33} (nF/m)	13.3	–
Tip mass (kg) = 0.012		

Table 4
Short-circuit and open-circuit resonance frequencies of bimorph cantilever without a tip mass.

First resonance frequency	VAM	Experiment Erturk Phd Thesis [2009]	% Error
f_1^{sc} (short circuit) [Hz]	509.79	502.50	1.43
f_1^{oc} (open circuit) [Hz]	523.26	524.70	0.2751

completely based on slender beam type energy harvester so to keep a perfect analogy between the experiment and our analysis we have used reduced material properties as mentioned in Table 3. The best approach would have been to model the structure using a strip like analysis. A comparison of short circuit and open circuit frequencies with experiments, for a biomorph cantilever without a tip mass is done in Table 4.

In Fig. 4 we can observe the first three coupled axial and bending modes corresponding to the first three natural frequencies. The performance of a harvester at resonance frequency is the main concern as its gives the maximum power output. The voltage FRF as defined in equation (61) is basically the voltage output per base acceleration. Fig. 5 shows the validation of voltage FRF as well as the validation of the tip velocity FRF with the experimental work done by Erturk et al. for different values of load resistances varying from a very low values, mid value to a very high value. The experimental short circuit resonance frequency is 45.6 Hz and our present analysis predicts it to be 46 Hz.

There is a frequency shift observed from 46 Hz to 48.2 Hz for the present theory for all the voltage FRF, tip velocity FRF, current FRF and power FRF when the load resistance is varied from 1 kΩ to 100 MΩ and has been shown in Fig. 6. The voltage output increases and the current output decreases as the load resistance vary from a low value to a high value. The present model is sensitive enough to capture all necessary parameters with variation in load resistance. The electric current FRF exhibits an opposite behaviour of that of the voltage FRF with change in load resistance. The pattern in the electrical power FRF with varying load resistance does not follow any trend as it is multiplication of voltage and current FRFs which are having opposite trends. For a given excitation frequency there is a particular value of load resistance that generates maximum power. The tip velocity FRFs intersects each other with change in load resistance. The short circuit and the open circuit frequency of the first mode are defined as the two extreme load condition which are

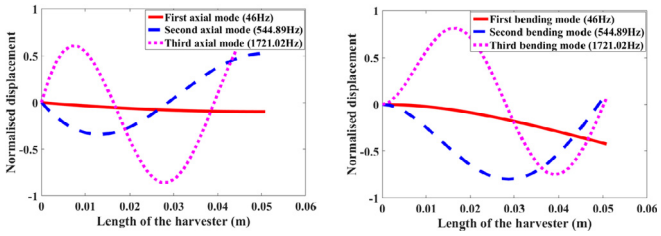

Fig. 4. Coupled axial, bending mode shapes corresponding to first, second and third natural frequency.

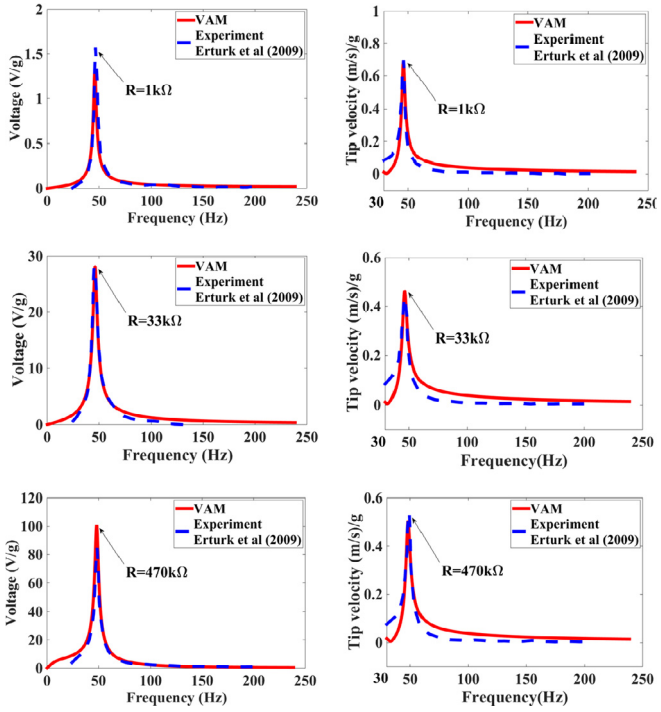

Fig. 5. VAM and experimental voltage and corresponding tip velocity FRF comparison for 1 kΩ, 33 kΩ and 470 kΩ load value.

predicted as 46 Hz and 49.27 Hz from the present model. The electromechanical coupling and the equivalent capacitance term are replaced to get the voltage, tip velocity, current and power FRFs for parallel connection case. The circuit representation of a series

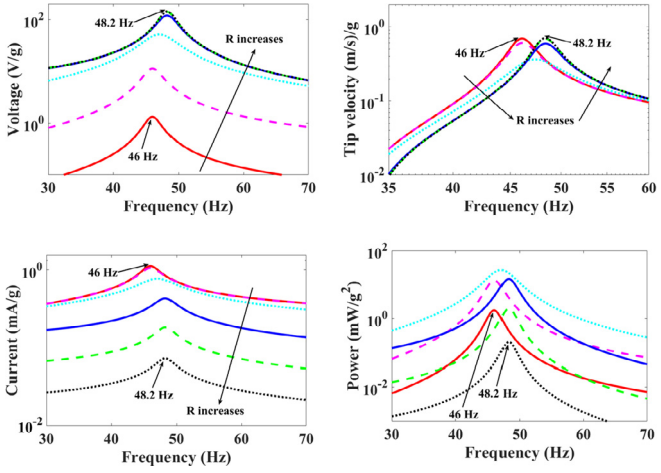

Fig. 6. Voltage, tip velocity, current and power FRF obtained from VAM for load resistance varying from 1 kΩ, 10 kΩ, 100 kΩ, 1 MΩ, 10 MΩ to 100 MΩ.

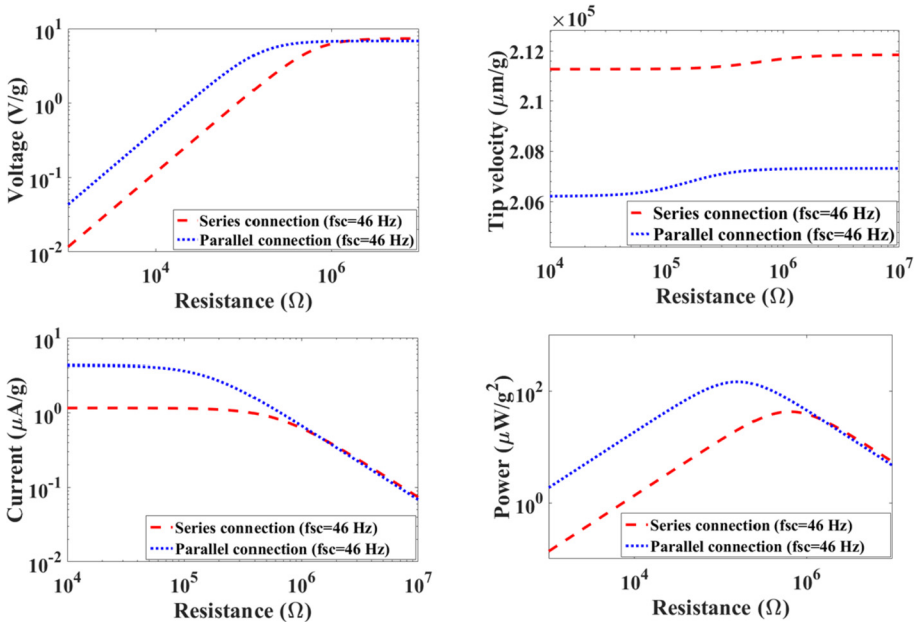

Fig. 7. Voltage, tip velocity, current and power with varying resistance for first mode for both series and parallel connection.

and parallel connection for a bimorph energy harvester has been shown in Fig. 3. The representation of electric field results in different mechanical equations for series and parallel connections of piezo layers. The voltage across the electrodes of each piezo layer is $\frac{\phi(t)}{2}$ for series connection whereas $\phi(t)$ for parallel connection. Also in series connection the poling direction of piezo layers are opposite to each other whereas it is same for parallel connection. Tabular comparison of the electromechanical parameters for series and parallel connections are shown in Table 2. Series connection generates larger voltage as compared to parallel and parallel connection generates larger current as compared to series after a certain load value. The maximum power outputs for a series and parallel connection case is identical only for a particular value of resistive load. From Fig. 7 we can observe that piezoelectric energy harvesters are poor current generators, whereas the level of voltage is fairly good which is useful for charging a battery. The poor level of current output will make the duration of charging long compared to the other commercially available battery chargers. Power output and tip velocity comparison for series and parallel connection for a particular frequency has been shown in Fig. 7. These all studies strengthen Variational asymptotic method (VAM) as a reliable and accurate modeling technique for any type of energy harvesters.

10. Summary and conclusions

This paper presents an asymptotically correct piezoelectric energy harvester model under base excitation and experimentally validates it. The advantage of using this mathematical model is that it can analyse an energy harvester made up of anisotropic material and can capture structural coupling and its effect on the harvester response. The present work also develops a single common platform to study a beam type PZT harvester working in extension, torsion, bending or any other combinations of these modes because of structural coupling. The present model can accommodate geometrical features like arbitrary shape of the cross-section, multilayer active inclusion. These are design parameters which are currently not possible to explore by any single harvester model currently existing in the literature. The present work lays a unifying platform for these and leaves options for incorporating other design parameters like taper, pre-twist and pre-curvature in future.

Acknowledgement

The first author would like to acknowledge MHRD, India for her PhD fellowship.

References

[1] DuToit NE, Wardle BL, Kim SG. Design consideration for MEMS scale piezoelectric mechanical vibration energy harvesters. Integrated Ferroelectrics 2005;71:121–60.
[2] Williams CB, Yates RB. Analysis of a micro-electric generator for microsystems. Sensor Actuator A 1996;52:8–11.
[3] Anton SR, Sodano HA. A review of power harvesting using piezoelectric materials (2003-2006). Smart Mater Struct 2007;16:R1–21.
[4] Zhu D, Tudor MJ, Beeby SP. Strategies for increasing the operating frequency range of vibration energy harvesters: a review. Meas Sci Technol 2010;21, 022001.
[5] Erturk A, Inman DJ. Piezoelectric energy harvesting Wiley. 2011.
[6] Erturk A, Inman DJ. On mechanical modeling of cantilevered piezoelectric vibration energy harvesters. J Intell Mater Syst Struct 2008;19:1311–25.
[7] Erturk A, Inman DJ. A distributed parameter electromechanical model for cantilevered piezoelectric energy harvesters. J Vib Acoust 2008;130:1–15.
[8] Erturk A, Inman DJ. An experimentally validated bimorph cantilever model for piezoelectric energy harvesting from base excitations. Smart Mater Struct 2009;18:1–18.
[9] Aladwani A, Arafa M, Aldraihem O, Baz A. Cantilevered piezoelectric energy harvester with a dynamic magnifier. J Vib Acoust 2012;134:1–10.
[10] Kim M, Hoegen M, Dugundji J, Wardle BL. Modeling and experimental verification of proof mass effects on vibration energy harvester performance. Smart Mater Struct 2010;19:1–21.
[11] Wang H, Meng Q. Analytical modeling and experimental of vibration-based piezoelectric bimorph beam with a tip-mass for power harvesting. Mech Syst Signal Process 2013;36:193–209.
[12] Azizi S, Ghodsi A, Jafari H, Ghazavi MR. A conceptual study on the dynamics of a piezoelectric MEMS (Micro Electro Mechanical System) energy harvester. Energy 2016;96:495–506.
[13] Lin HC, Wu PH, Lien IC, Shu YC. Analysis of an array of piezoelectric energy harvesters connected in series. Smart Mater Struct 2013;22, 094026.
[14] Adhikari S, Friswell MI, Inman DJ. Piezoelectric energy harvesting from broadband random vibrations Smart. Mater Struct 2009;18:1–7.
[15] Hagood NW, Chung WH, Flotow AV. Modelling of piezoelectric actuator dynamics for active structural control. J Intell Mater Syst Struct 1990;1:327–54.
[16] Lu F, Lee HP, Lim SP. Modeling and analysis of micro piezoelectric power generators for micro-electromechanical-systems applications. Smart Mater Struct 2004;13:57–63.
[17] Zhu M, Worthington E, Njuguna J. Analyses of power output of piezoelectric energy harvesting devices directly connected to a resistive load using a

coupled piezoelectric circuit finite element method IEEE Transactions on Ultrasonics. Ferroelectrics and Frequency Control 2009;56:1309–17.
[18] Junior CDM, Erturk A, Inman DJ. An electromechanical finite element model for piezoelectric energy harvester plates. J Sound Vib 2009;327:9–25.
[19] Yang Y, Wu H, Soh CK. Experiment and modeling of a two-dimensional piezoelectric energy harvester. Smart Mater Struct 2015;24(12):125011.
[20] Hajati A, Kim SG. Ultra-wide bandwidth piezoelectric energy harvesting. Appl Phys Lett 2011;99, 083105.
[21] Halim MA, Park JY. Theoretical modeling and analysis of mechanical impact driven and frequency up-converted piezoelectric energy harvester for low-frequency and wide-bandwidth operation. Sensor Actuator A 2014;208:56–65.
[22] Jeong S, Cho JY, Sung TH, Yoo HH. Electromechanical modeling and power performance analysis of a piezoelectric energy harvester having an attached mass and a segmented piezoelectric layer. Smart Mater Struct 2017;26(3):035035.
[23] Lefeuvre E, Badel A, Brenes A, Seok S, Yoo CS. Power and frequency bandwidth improvement of piezoelectric energy harvesting devices using phase-shifted synchronous electric charge extraction interface circuit. J Intell Mater Syst Struct 2017. 1045389X17704914.
[24] Xie XD, Carpinteri A, Wang Q. A theoretical model for a piezoelectric energy harvester with a tapered shape. Eng Struct 2017;144:19–25.
[25] Abdelmoula H, Zimmerman S, Abdelkefi A. Accurate modeling, comparative analysis, and performance enhancement of broadband piezoelectric energy harvesters with single and dual magnetic forces. Int J Non Lin Mech 2017;95:355–63.
[26] Hu G, Tang L, Das R, Marzocca P. A two-degree-of-freedom piezoelectric energy harvester with stoppers for achieving enhanced performance. Int J Mech Sci 2017.
[27] Berdichevsky VL. Variational asymptotic method of constructing a theory of shells. PMM 1979;43:664–87.
[28] Yu W, Hodges DH. Elasticity solutions versus asymptotic sectional analysis of homogeneous, isotropic, prismatic beams. J Appl Mech 2004;71:15–23.
[29] Yu W. Variational asymptotic modeling of composite dimensionally reducible structures. PhD thesis. Georgia Institute of Technology; 2002.
[30] Roy S, Yu W, Han D. An asymptotically correct classical model for smart beams. Int J Solid Struct 2007;44:8424–39.
[31] Roy S, Yu W. Dimensional reduction of a piezoelectric composite rod European. J. Mech. A Solids 2009;28:368–76.
[32] Banerjee S, Roy S. Multiphysics analysis of an asymptotically correct piezoelectric sensor under static and dynamic load. Int J Solid Struct 2016;92–93:64–75.
[33] Hodges DH. Nonlinear composite beam theory AIAA Washington DC. 2006.